Available online at www.sciencedirect.com
SCIENCE DIRECT®
International Journal of Solids and Structures 42 (2005) 1055–1072
INTERNATIONAL JOURNAL OF SOLIDS and STRUCTURES
www.elsevier.com/locate/ijsolstr

Steam pressure induced in crack-like cavities in moisture saturated polymer matrix composites during rapid heating

Chung-Yuen Hui [a,*], Vijayanand Muralidharan [a], Michael O. Thompson [b]

[a] Department of Theoretical and Applied Mechanics, Cornell University, 236 Thurston Hall, Ithaca, NY 14853, USA
[b] Department of Material Science and Engineering, Cornell University, Ithaca, NY 14853, USA

Received 3 March 2004; received in revised form 17 June 2004
Available online 18 September 2004

Abstract

The time history of steam pressure inside an isolated "crack-like" micro-cavity in a polymer matrix composite is studied by assuming that the chemical potential of water is continuous across the cavity/polymer interface. Steam pressure inside the cavity is due to rapid heating of moisture-saturated composites from its initial temperature to a final temperature T_f. Exact closed form solutions are obtained for a "crack-like" cavity inside an infinite and a finite plate. For the case of an infinite plate, the exact solution shows that the steam pressure approaches the saturated steam pressure $p_{sat}(T_f)$ at a characteristic time $t_c \cong \frac{25h^2}{D_f}\left(\frac{M_w p_{sat}(T_f)}{RT_f\psi_0}\right)^2$, where h is the cavity height, D_f is the diffusivity of water at T_f, M_w is the molecular weight of water, ψ_0 is the initial moisture concentration of the composite and R is the universal gas constant. When moisture is allowed to escape from the composite, such as in the case of a finite plate, the maximum steam pressure depends on a single dimensionless parameter $\alpha = \frac{LRT_f\psi_0}{hM_w p_{sat}(T_f)}$, where L is the thickness of the composite plate. For large α, the maximum steam pressure approaches $p_{sat}(T_f)$. However, the maximum steam pressure can be significantly less than $p_{sat}(T_f)$ when $\alpha \leqslant 4$. The present model can also be used to study the 'popcorning' observed in electronic packages.

1. Introduction

Due to their high specific stiffness and strength properties at temperatures in excess of 300 °C, graphite fiber/polyimide matrix composites represent an important class of materials for secondary support structures in reusable launch vehicles. When not in service, these composites can absorb moisture in excess of

* Corresponding author. Tel.: +1 607 255 9174; fax: +1 607 255 2011.
E-mail addresses: ch45@cornell.edu (C.-Y. Hui), vm45@cornell.edu (V. Muralidharan), mot1@cornell.edu (M.O. Thompson).

0020-7683/$ - see front matter © 2004 Elsevier Ltd. All rights reserved.
doi:10.1016/j.ijsolstr.2004.06.058

Nomenclature

ψ	moisture concentration
ψ_0, ψ_∞	initial and equilibrium moisture concentration respectively
T_0, T_f	initial and final temperature respectively
$D(T)$, D_f	moisture diffusivity at temperatures T and T_f respectively
χ	relative humidity
μ_p, μ_{air}	chemical potential of water in polymer and air respectively
$\dot{T}$	heating rate
n_0, n	initial and final number of moles of water per unit projected area in the cavity
p	partial pressure of water vapor in the cavity
$p_{sat}(T)$	saturated vapor pressure of pure water at temperature T
L, h	plate thickness and cavity depth respectively
k	Henry's constant
ϕ	normalized concentration
$\bar{x}$, X	normalized position
$\bar{t}$, τ	normalized times
L_d	thickness of depletion layer
M_w	molecular weight of water, 18 g/mol
R	gas constant, 8.314 J/(mol K)
d	dimensionless parameter, $d = \frac{RT_0\psi_0}{M_w p_{sat}(T_0)}$
c	dimensionless parameter in the finite plate problem, $c = 1-\psi_\infty/\psi_0$
α	dimensionless parameter in the finite plate problem, $\alpha = \frac{LRT_f\psi_0}{hM_w p_{sat}(T_f)}$

3% by weight from the environment. During service, they can be subjected to heating rates as high as 100 °C/s. At such heating rates, failure or extensive internal damage of the composite can occur due to steam induced delamination and blistering. This phenomenon has led to many studies on blister initiation and growth in high temperature resins and composites (see Bowman et al., 2001; Price et al., 1995; Rice, 1996; Rice and Lee, 1997; Shirrel, 1978). For example, Rice and Lee (1997) have conducted weight loss experiments by subjecting polyimide plates to various heating rates. From these experiments, they determine the dependence of the moisture diffusivity of water on temperature. They also studied the onset of blisters by measuring the change of thickness of the composite plate during heating. By observing that the volume of their samples actually increases when heated at a constant external pressure of 10 MPa, they concluded that the pressure inside the steam filled cavities must exceed 10 MPa. A detailed study of the internal steam pressure caused by the effusion of water in carbon phenolic composites was carried out by Sullivan and Stokes (1997) using a theory of gas flow in a rigid porous media.

The issue of moisture absorption and subsequent delamination is also important to the electronic packaging community. When polymer-encapsulated microcircuits are exposed to high temperatures during infra-red reflow soldering, a sound characteristic of popcorn popping is detected. This so-called 'popcorning' effect is due to the moisture induced delamination at the package interfaces. For more details, the readers are referred to the articles by McCluskey et al. (1997), Gannamani and Pecht (1996) and the references therein.

Blister formation and interlaminar crack growth are controlled by moisture transport from the polymer to microcavities in the composite. A simple problem is to consider the time history of steam pressure inside an isolated cavity in a moisture-saturated composite. During heating, water molecules are transported from

the polymer into the cavity, resulting in an increase of steam pressure. On the other hand, since moisture can also escape from the surfaces of the composite; the pressure inside the cavity can be reduced if the composite is sufficiently thin. The following questions naturally arise: How fast does the pressure build up inside a cavity? In addition, how does steam pressure depend on the cavity size, the moisture diffusivity, the heating rate and the moisture content in the composite before heating? A micromechanical model addressing these questions will allow us to quantify the time dependent driving force causing damage and can be used to study the interactions between cavities and other forms of damages, such as interfacial cracks. Such a model can eventually lead to a micromechanical based continuum model for damage evolution in a composite.

There is a vast literature on the diffusion of moisture in polymers and polymer composites. The focus of these studies is to predict the moisture concentration as a function of position and time in a homogenized composite and in neat resins. Much less attention is given to micromechanical modeling of blister formation. For polymers and polymer composites, readers are referred to a collection of articles edited by Springer (1981). In general, the diffusivity of moisture is stress, concentration and temperature dependent (for example, see Weitsman, 1987). Despite the many theoretical and experimental developments, there is still no consensus on the relative importance of these effects. In addition, experiments seem to suggest that moisture transport is very sensitive to the amount of internal damage (Shirrel, 1978). Such damage can occur during fabrication or when the composite is exposed to moist air with high relative humidity and high ambient temperatures (Loos and Springer, 1981; Shirrel, 1978; Whitney and Browning, 1978). Damage occurs even at zero heating rates with no applied mechanical load. Current theories on moisture transport do not take into account the development of internal damage. Despite these complications, weight gain experiments on composite plates exposed to moist air with a fixed relative humidity have shown that moisture diffusion data can be fitted using a concentration dependent form of Fick's law (Shirrel, 1978; Whitney and Browning, 1978). In particular, when composite damage is low, the diffusivity is found to be concentration independent (Whitney and Browning, 1978). A further simplification is to note that the thermal diffusivity of typical composites is much larger than the moisture diffusivity, so that thermal equilibrium is attained much faster than moisture equilibrium. Thus, the thermal conduction problem and the moisture diffusion problem can be decoupled.

Although Fick's law has been used quite successfully to interpret weight gain experiments, there are some shortcomings. Fick's law states that the moisture flux is proportional to the concentration gradient, whereas in reality, it is the gradient of the chemical potential of moisture that drives diffusion. A formulation of transport driven entirely by concentration gradient has limitations; even in one-dimensional weight gain calculations. For example, consider a long plate of thickness L with an initial moisture concentration of ψ_0. The moisture concentration is defined as the mass of water per unit volume of composite. The top and bottom surfaces of the plate are located at $x = 0$ and $x = L$ respectively. The plate is exposed to moist air at a constant temperature T with a fixed relative humidity χ. The moisture concentration inside the plate, ψ, satisfies the diffusion equation

$$\frac{\partial \psi}{\partial t} = D\frac{\partial^2 \psi}{\partial x^2} \tag{1}$$

where x is the coordinate normal to the plate and D is the diffusivity of water. The difficulty lies in determining the boundary conditions on $x = 0$ and $x = L$. The boundary condition often used in the literature (Shirrel, 1978; Whitney and Browning, 1978) is:

$$\psi(x = 0, t > 0) = \psi(x = L, t > 0) = \psi_\infty \tag{2}$$

where ψ_∞ is the equilibrium concentration. From the experimental point of view, this boundary condition presents no difficulty, since ψ_∞ can be determined from the weight gained at long times. However, this boundary condition is inadequate from a modeling standpoint as it should be related to the relative

humidity since exposing the polymer plate to moist air drives moisture transport. Indeed, experiments have shown that ψ_∞ is related to the relative humidity χ by (Shirrel, 1978; Whitney and Browning, 1978):

$$\psi_\infty = A(T)\chi \tag{3a}$$

but some authors (Deiasi and Whiteside, 1978; Woo and Piggott, 1987) have observed a relationship of the form

$$\psi_\infty = A(T)\chi^b \tag{3b}$$

where the exponent b is different from one. It is not clear whether the difference in exponent b is because of an experimental error as pointed by Loos and Springer (1981) or is actually present in some material systems. In addition, the dependence of $A(T)$ on temperature is found to be very weak (Loos and Springer, 1981). This paradox can be resolved by using the approach of Sullivan and Stokes (1997) by assuming that the water molecules on the surface of the polymer composite are in local chemical equilibrium with the surrounding moist air, i.e.

$$\mu_{\mathrm{p}}(x=0,t) = \mu_{\mathrm{air}} \tag{4}$$

where μ_{p}, μ_{air} denote the chemical potential of the water in the polymer and water in the surrounding air respectively. The chemical potential of the water in the polymer composite is a function of the time and position, whereas the chemical potential of water in the air is spatially uniform and depends only on the relatively humidity χ and the temperature, i.e.,

$$\mu_{\mathrm{air}} = \mu_0(T) + RT\ln\chi \tag{5}$$

where $\mu_0(T)$ is the chemical potential of pure water at temperature T. As in Sullivan (1996), the water and the polymer composite are treated as a binary mixture. The chemical potential of the water in the polymer composite can be expressed in terms of the activity of the water, a:

$$\mu_{\mathrm{p}} = \mu_0(T) + RT\ln a(x=0,t>0) \tag{6}$$

At *sufficiently* small concentrations, Henry's law is valid, that is:

$$a(x=0,t>0) = k(T)\psi(x=0,t>0) \tag{7}$$

Therefore, local equilibrium implies that

$$\psi(x=0,t>0) = \chi/k(T)$$

This equation is the same as (3a) provided that $A(T)$ is identified with $1/k(T)$. This shows that the boundary condition (2) used in the literature is consistent with the chemical potential approach.

2. Problem statement

The geometry is shown schematically in Fig. 1. For simplicity, we consider a "crack-like" rectangular cavity in the mid-plane of a plate of thickness $2L + 2h$. Specifically, the lateral dimension of the cavity is assumed to be much greater than its thickness $2h$ so that moisture transport through the lateral walls of the cavity can be neglected. This assumption and symmetry allows us to study the one dimensional diffusion problem illustrated in Fig. 2.

Initially, the composite is in thermal equilibrium at temperature T_0. Let ψ_0 denote the initial moisture concentration in the composite. Without loss in generality, we assume that the composite is initially fully saturated, that is, the relative humidity inside the cavity is 100%. The composite is subjected to the following thermal history:

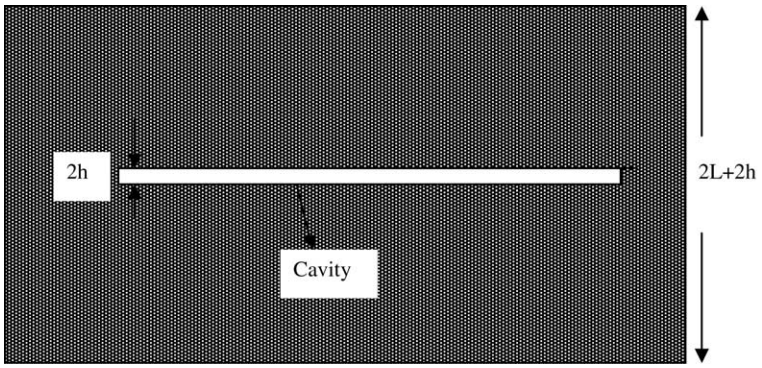

Fig. 1. A crack-like cavity in the mid-plane of a plate of thickness $2L$.

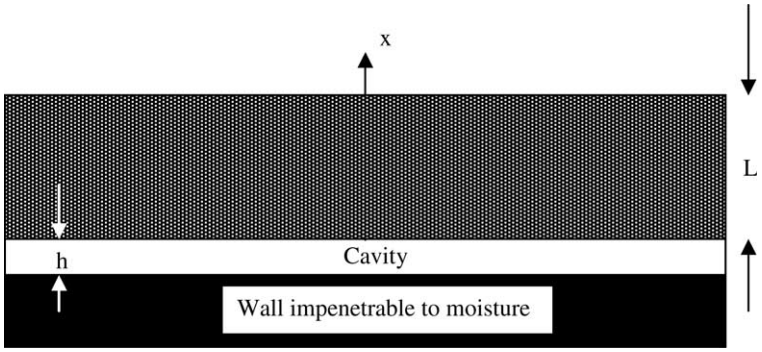

Fig. 2. Top half of the cavity and plate due to symmetry considerations.

$$T(t) = \begin{cases} T_0 + \dot{T}t & 0 \leqslant t \leqslant t_f \\ T_f & t \geqslant t_f \end{cases} \tag{8}$$

where

$$\dot{T} = \frac{T_f - T_0}{t_f} \tag{8a}$$

is the heating rate and t_f is the time taken to reach the temperature T_f. For simplicity, we assume that the composite is rigid so that the cavity is un-deformable. This assumption will overestimate the rate of pressure increase in the cavity. The validity of this assumption will be addressed in the discussion. To complete the problem formulation, the polymer and the water is treated as a binary solution. Since diffusion is driven by the gradient of chemical potential μ of the water instead of concentration gradient, the moisture flux, denoted by $\vec{J}$, is given by (Shewmon, 1989):

$$\vec{J} = -M\psi\nabla\mu \tag{9}$$

where M is the mobility of water molecules. Conservation of mass implies that

$$\nabla \cdot \vec{J} = -\partial\psi/\partial t \tag{10}$$

The governing equation for moisture diffusion is obtained by combining (9) and (10), i.e.,

$$\nabla \cdot (M\psi\nabla\mu) = \partial\psi/\partial t \tag{11}$$

3. Boundary conditions

To gain physical insight, consider the special case where the thickness of the composite plate is very large in comparison with the cavity height. In this case the moisture concentration far away from the cavity is given by

$$\psi(x \to \infty, t) = \psi_0 \tag{12}$$

The difficult boundary condition is associated with the cavity surface at $x = 0$. Local equilibrium implies that the chemical potential of water is continuous across the interface $x = 0$. Let μ_p and μ_c denote the chemical potential of water in the polymer and cavity respectively. The assumption of local equilibrium implies that:

$$\mu_p(x = 0^+) = \mu_c \tag{13}$$

The chemical potential of water in the cavity is given by (5),

$$\mu_c = \mu_0(T) + RT \ln \frac{p}{p_{sat}(T)} \tag{14}$$

where p is the partial pressure of water vapor in the cavity and $p_{sat}(T)$ is the saturated vapor pressure of pure water at temperature T. Assuming Henry's law, local equilibrium and (5)–(7) implies that

$$k(T)\psi(x = 0, t) = \frac{p}{p_{sat}(T)} \tag{15}$$

The steam pressure inside the cavity is related to the cavity height h by the ideal gas law,

$$p = \frac{nRT}{h} \tag{16}$$

where n is the number of moles of water per unit projected area of the cavity. It is related to the moisture flux through the polymer surface, J, by

$$n = n_0 - \frac{1}{M_w} \int_0^t J(x = 0, t')\, dt' \tag{17}$$

where M_w is the molecular weight of water and n_0 is the initial number of moles of water per unit projected area inside the cavity and is given by

$$n_0 = \frac{p_{sat}(T_0)h}{RT_0} \tag{18}$$

The second term in (17) is the total number of moles of water inside the cavity due to diffusive transport across the interface $x = 0$. Since initially the composite is fully saturated, $k(T_0)\psi(x = 0, t = 0) = 1$ or $k(T_0) = 1/\psi_0$. Combining (15)–(18), the boundary condition on the interface $x = 0$ is:

$$k(T)\psi(x = 0, t) = \frac{T}{p_{sat}(T)} \left(\frac{p_{sat}(T_0)}{T_0} + \frac{R}{M_w h} \int_0^t D(T(t'))\psi_{,x}(x = 0, t')\, dt' \right) \tag{19}$$

Henry's law and (9) implies that

$$J = -MRT\, \partial\psi/\partial x \equiv -D\, \partial\psi/\partial x \tag{20}$$

where $D = MRT$ is the diffusivity. Thus, the Henry's law assumption leads to the linear diffusion equation,

$$D(T)\, \partial^2\psi/\partial x^2 = \partial\psi/\partial t \tag{21}$$

It is to be noted that D is a function of temperature. Since temperature is a function of time, D is also time dependent. The next step is to specify the behavior of $k(T)$, $p_{\text{sat}}(T)$ and $D(T)$.

Weight gain experiments have shown that $k(T)$ is quite insensitive to temperature (Deiasi and Whiteside, 1978; Loos and Springer, 1981; Shirrel, 1978). Consistent with these observations, we assume

$$k(T) = k(T_0) = 1/\psi_0. \tag{22}$$

The saturated vapor pressure of water can be obtained from steam tables. $p_{\text{sat}}(T)$ is well approximated by the equation:

$$p_{\text{sat}}(T) = P_0 \exp\left(\frac{-\widetilde{T}}{T}\right) \tag{23}$$

where $P_0 = 36839.35$ MPa, $\widetilde{T} = 4802.4$ K. Eq. (23) can be rewritten as

$$p^*_{\text{sat}}(T^*) = \exp\left(\widetilde{T}^*\left(1 - \frac{1}{T^*}\right)\right) \tag{24}$$

where $p^*_{\text{sat}}(T^*) = p_{\text{sat}}(T)/p_{\text{sat}}(T_0)$ and $\widetilde{T}^* \equiv \widetilde{T}/T_0$. Fig. 3 plots $p^*_{\text{sat}}(T)$ versus $T^* \equiv T/T_0$. Experiments have also shown that the dependence of diffusivity on temperature obey an Arrhenius equation of the form (Rice and Lee, 1997; Whitney and Browning, 1978; Woo and Piggott, 1987) which can be written as

$$\frac{D(T)}{D(T_0)} = \exp\left(\widetilde{T}^{**}\left(1 - \frac{1}{T^*}\right)\right) \tag{25}$$

where T^{**} is a material constant. For example, for the material AFR700B, which is a high-temperature fluorinated polyimide, Rice and Lee (1997) reported a $T^{**} \approx 13.7$.

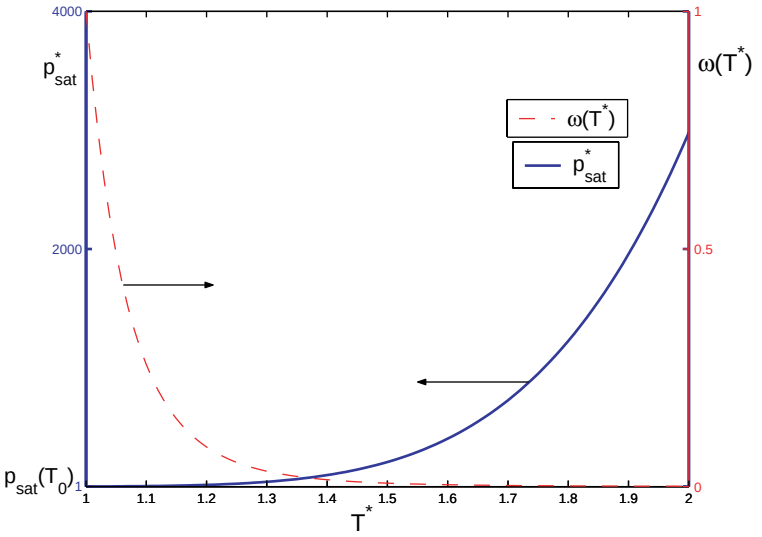

Fig. 3. Plot of $p^*_{\text{sat}}(T)$ and $\omega(T^*)$ versus normalized temperature T^*. Arrows point to the appropriate axis labels.

4. Method of solution

Introducing the dimensionless variables

$$\phi = \psi/\psi_0 \tag{26a}$$

$$\bar{x} = x/h \tag{26b}$$

and normalized time,

$$\bar{t} = \frac{1}{h^2}\int_0^t D(T(t'))\,\mathrm{d}t', \tag{26c}$$

(21) can be reduced to the standard form

$$\partial\phi/\partial\bar{t} = \partial^2\phi/\partial\bar{x}^2 \quad \bar{x} > 0 \tag{27}$$

The boundary conditions become:

$$\phi(\bar{x}=0,\bar{t}>0) = \omega(T^*)\left[1 + d\int_0^{\bar{t}} \phi_{,\bar{x}}|_{\bar{x}=0}\,\mathrm{d}\bar{t}'\right] \tag{28}$$

and

$$\phi(\bar{x}\to\infty,\bar{t}>0) = 1 \tag{29}$$

where

$$d = \frac{RT_0\psi_0}{M_{\mathrm{w}}p_{\mathrm{sat}}(T_0)} \tag{30}$$

$$\omega(T^*) = \frac{T^*}{p^*_{\mathrm{sat}}(T^*)} \tag{31}$$

Using T_0=300 K, ψ_o=42 kg/m^3, and (23), we get $d \approx 1400$. The function $\omega(T^*)$ is in general time dependent. The initial condition is

$$\phi(\bar{x},\bar{t}=0) = 1 \tag{32}$$

5. Infinitely thick plate with infinitely fast heating

To simplify the problem further, we consider the limiting case of very high heating rates, i.e. $\dot{T}\to\infty$. This is an important case since it provides an upper limit on how fast the pressure can build up. Since the heating rate is infinite, we have

$$T = \begin{cases} T_0 & t = 0 \\ T_{\mathrm{f}} & t = 0^+ \end{cases} \tag{33}$$

Note that in this case $\bar{t} = D_{\mathrm{f}}t/h^2$. In addition, the governing Eq. (27) and the boundary and initial conditions (28), (29), (32) remain unchanged provided that the time dependent dimensionless function (31) in (28) is replaced by the constant

$$\omega_{\mathrm{f}} = \frac{T^*_{\mathrm{f}}}{p^*_{\mathrm{sat}}(T^*_{\mathrm{f}})} \tag{34}$$

which is typically much smaller than one. For example, $\omega_f = 6.7 \times 10^{-4}$ for $T_0 = 300$ K and $T_f = 600$ K. All the examples in this paper (e.g. Figs. 3–8) are based on $T_0 = 300$ K and T_f=600 K. A plot of $\omega(T^*)$ versus normalized absolute temperature is shown in Fig. 3.

For the case of infinitely fast heating, we normalize the equations using a new set of dimensionless variables X and τ i.e.,

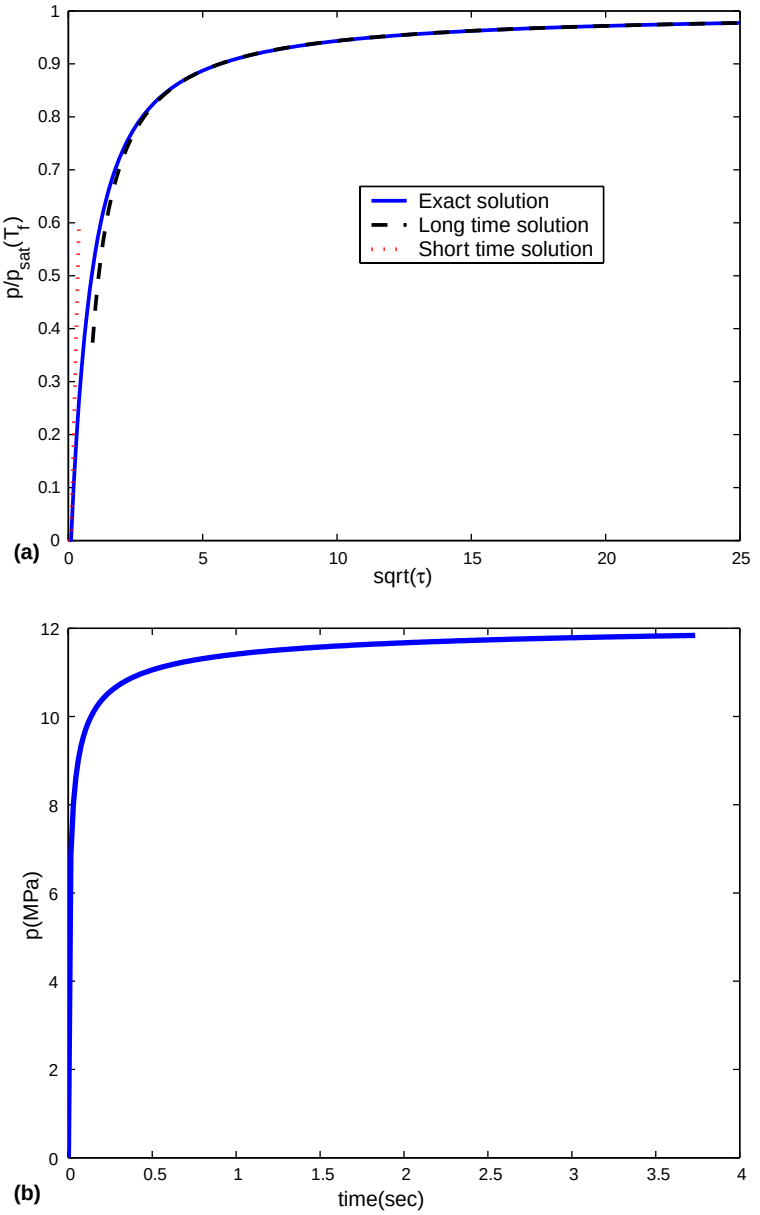

Fig. 4. (a) Plot of normalized pressure with the square root of normalized time. (b) Plot of pressure in cavity versus real time.

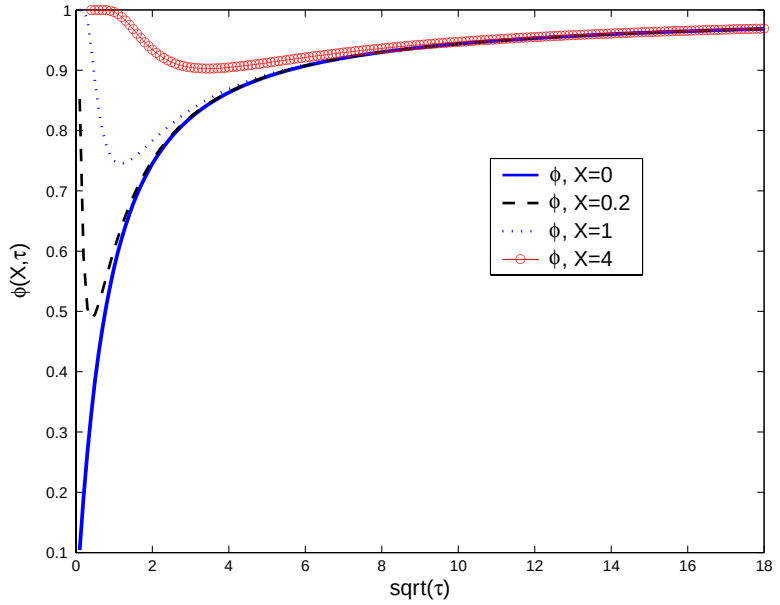

Fig. 5. Plot of normalized concentration with the square root of normalized time for different normalized distances from the cavity surface.

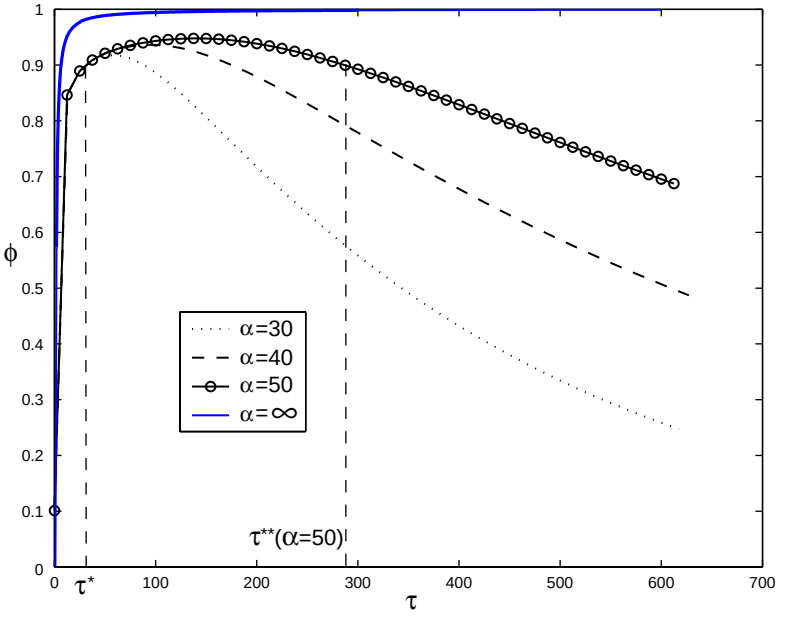

Fig. 6. Plot of normalized moisture concentration on the cavity surface with the normalized time τ for different α.

$$X = \frac{d\omega_f}{h}x, \quad \tau = \frac{d^2\omega_f^2 D_f}{h^2}t \tag{35}$$

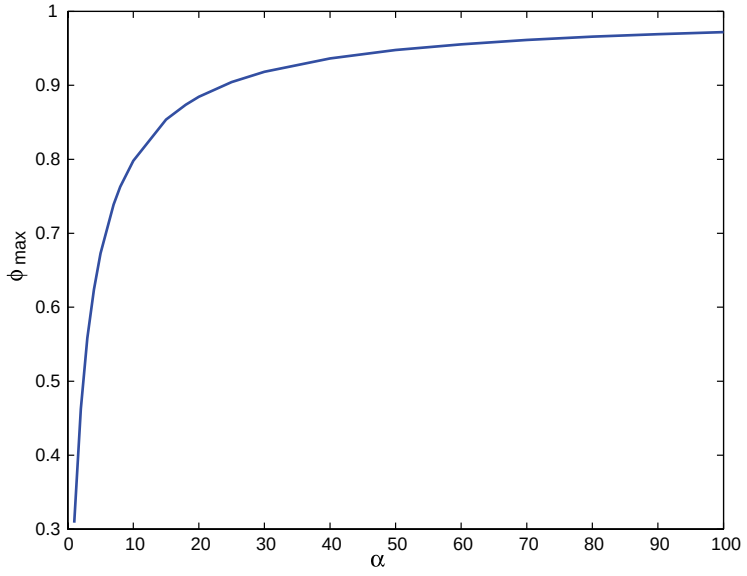

Fig. 7. Plot of maximum normalized moisture concentration on the cavity surface with the parameter α.

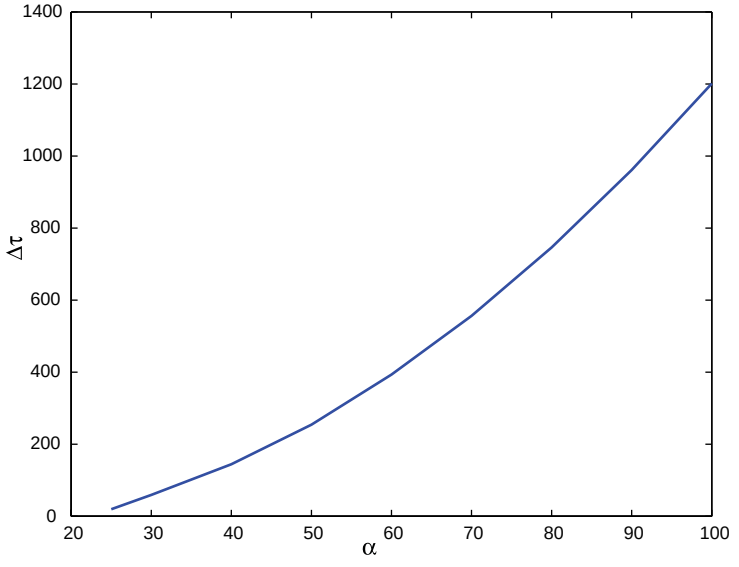

Fig. 8. Dependence of the duration of high pressure, $\Delta\tau$ with α.

Also, it is convenient to introduce the function $g = 1-\phi$. Eq. (27) remains unchanged with this transformation, i.e.

$$\partial g/\partial \tau = \partial^2 g/\partial X^2 \tag{36}$$

whereas the boundary conditions become:

$$1 - g(X = 0, \tau > 0) = \omega_f - \int_0^\tau \frac{\partial g}{\partial X}(X = 0, \tau')\, d\tau' \tag{37a}$$

and

$$g(X \to \infty, \tau > 0) = 0 \tag{37b}$$

The new initial condition is

$$g(X, \tau = 0) = 0 \tag{37c}$$

Taking the Laplace transform of (36), we obtain

$$\tilde{g}(X, s) = A(s) e^{-\sqrt{s}X} \tag{38}$$

where

$$\tilde{g}(X, s) = \int_0^\infty e^{-s\tau} g(X, \tau)\, d\tau \tag{39}$$

denotes the Laplace transform of g. The function $A(s)$ is determined by the Laplace transform of (37a). A simple calculation shows that

$$A(s) = \frac{1 - \omega_f}{\sqrt{s}(\sqrt{s} + 1)}. \tag{40}$$

The function $1 - g(X = 0,t) = \phi(X = 0,t)$ is important, since it is the time history of the normalized pressure inside the cavity. Indeed, from (15),

$$1 - g(X = 0, \tau) = p(X = 0, \tau)/p_{sat}(T_f) \tag{41}$$

Since $A(s) = \tilde{g}(X = 0, s)$, the steam pressure inside the cavity is given by:

$$p(X = 0, \tau) = p_{sat}(T_f)[1 - \ell^{-1}(A(s))] \tag{42}$$

where ℓ^{-1} denote the inverse Laplace transform operator. Since

$$\ell^{-1}(A(s)) = (1 - \omega_f) e^\tau \operatorname{erfc} \sqrt{\tau},$$

the time history of the steam pressure in the cavity is

$$p(X = 0, \tau) = p_{sat}(T_f)[1 - (1 - \omega_f) e^\tau \operatorname{erfc} \sqrt{\tau}] \tag{43}$$

The short and long time behavior of the steam pressure can be obtained using the asymptotic behavior of the complementary error function, it is found to be:

$$p(X = 0, t) = p_{sat}(T_0)(T_f/T_0)\left[1 + 2(1 - \omega_f)\frac{d}{h}\sqrt{D_f t}\right], \quad \frac{d\omega_f\sqrt{\pi D_f t}}{h} \ll 1 \tag{44}$$

$$p(X = 0, t) = p_{sat}(T_f)\left[1 - (1 - \omega_f)\frac{h}{d\omega_f\sqrt{\pi D_f t}}\right], \quad \frac{d\omega_f\sqrt{\pi D_f t}}{h} \gg 1 \tag{45}$$

where these asymptotic results are expressed in physical time. Eq. (44) shows that the pressure jumps from $p_{sat}(T_0)$ from $t = 0$ to $p_{sat}(T_0)(T_f/T_0)$ at $t = 0^+$. This sudden jump is due to the infinite heating rate, which cause the temperature to jump from T_0 to T_f. Since steam is modeled as an ideal gas and the cavity is rigid, the pressure increases instantaneously by the factor T_f/T_0 (Boyle's Law). However, this increase in pressure is insignificant in comparison with the saturated steam pressure at T_f. For example, if a moisture-saturated

composite, initially at room temperature $T_0 = 300$ K is rapidly heated to its glass transition temperature, which is about 625 K for high temperature polyimide, (44) implies that the sudden jump in vapor pressure inside a cavity is about a factor two above the saturated vapor pressure at room temperature, $p_{sat}(T_0)$. This increase is insignificant in comparison with the final saturated steam pressure at $T_f = 625$ K, which is about 4000 times $p_{sat}(T_0)$.

Fig. 4a plots the normalized steam pressure $p(X = 0,\tau)/p_{sat}(T_f)$ versus the square root of the normalized time τ. The short time solution (44) and the long time solution (45) are also plotted on the same figure. The maximum pressure $p_{sat}(T_f)$ is reached at a normalized time corresponding to $\sqrt{\tau} \approx 10$. Fig. 4a shows that the characteristic normalized time τ_c for the transition from short time to long time behavior is $\sqrt{\tau_c} \simeq 5$; in real times, this is

$$t_c \cong \frac{25h^2}{D_f}\left(\frac{M_w p_{sat}(T_f)}{RT_f\psi_0}\right)^2 \tag{46}$$

For h=10 μm and $D_f = 6.82 \times 10^{-9}$ m^2/s (using (25) and Rice and Lee, 1997), the transition time t_c is about 0.4 s. Fig. 4b plots the actual pressure versus real time.

6. Depletion layer

Although the composite is infinitely thick in comparison with the depth of the cavity, the moisture inside the cavity is supplied from a thin layer of polymer adjacent to it. The thickness of this layer evolves with time. For short times, this layer increases with time as water is depleted. As the moisture is replenished by diffusion, the thickness of this layer goes down and finally vanishes when the cavity is fully pressurized. Mathematically, if we consider a fixed point $X > 0$ in the composite, the normalized moisture concentration $\phi(X,\tau)$ at that location would decrease from its initial value of one as moisture is transported to the cavity. The moisture concentration will eventually increase and will reach its initial value of one when the cavity is fully pressurized. Thus, for any fixed $X > 0$, $\phi(X,\tau)$ has a minimum $\phi_{min}(X)$ at some time $\tau_{min}(X)$. The thickness of the depletion layer, L_d, is defined by the condition

$$\phi_{min}(X_d) = 0.9 \tag{47}$$

where $X_d = L_d/h$. To evaluate L_d, we need to determine the moisture concentration as a function of position and time. The concentration can be obtained by inverting the inverse Laplace transform of $\tilde{g}(X,s)$. Using (38) and (40), it is

$$\phi(X,\tau) = 1 - (1-\omega_f)e^X e^\tau \operatorname{erfc}\left(\sqrt{\tau} + \frac{X}{2\sqrt{\tau}}\right) \tag{48}$$

It can be seen that (43) is recovered as $X \to 0$. The moisture concentration at different normalized distances from the cavity surface is plotted against the square root of the normalized time τ in Fig. 5. Fig. 5 shows that

$$\phi_{min}(X_d = 4) \simeq 0.9 \Rightarrow \frac{L_d}{h} \simeq 4 \tag{49}$$

Therefore, the depletion layer is about four times the cavity depth.

Since the plate is infinitely thick, steam can only enter the cavity and cannot escape. Thus, the maximum pressure is always $p_{sat}(T_f)$. The situation is different if the plate has a finite thickness. Indeed, for a sufficiently thin plate, the maximum steam pressure can be much less than $p_{sat}(T_f)$. Since the thickness of the depletion layer is about $4h$, for plates of thickness much larger than $4h$, the steam pressure can be significant and can reach the saturated pressure.

7. Finite plate thickness, infinitely fast heating

To demonstrate the validity of this argument and to study the dependence of the maximum steam pressure in the cavity as a function of plate thickness, we solve the finite plate problem. The governing equations are still given by (36, 37a, 37c). However, the boundary condition (37b) is replaced by

$$g(X=\alpha,\tau>0)=1-\psi_\infty/\psi_0=1-\phi_\infty\equiv c \tag{50}$$

where $\alpha=d\omega_f L/h$. This new boundary condition states that the external surface of the plate is in contact with dry air; where ψ_∞ is the long time moisture concentration of the plate and is assumed to be much smaller than ψ_0 so that $c\simeq 1$. Taking the Laplace transform of (36) and using (37c), we obtain

$$\tilde{g}(X,s)=A(s)e^{\sqrt{s}X}+B(s)e^{-X\sqrt{s}} \tag{51}$$

The functions $A(s)$, $B(s)$ are determined by the Laplace transform of (37a) and (50). They are found to be

$$A=\frac{\left(\frac{1-\omega_f}{s}\right)e^{-\alpha\sqrt{s}}-\left(1+\frac{1}{\sqrt{s}}\right)\frac{c}{s}}{\left(1-\frac{1}{\sqrt{s}}\right)e^{-\alpha\sqrt{s}}-e^{\alpha\sqrt{s}}\left(1+\frac{1}{\sqrt{s}}\right)} \tag{52}$$

$$B=\frac{\left(1-\frac{1}{\sqrt{s}}\right)\frac{c}{s}-\left(\frac{1-\omega_f}{s}\right)e^{\alpha\sqrt{s}}}{\left(1-\frac{1}{\sqrt{s}}\right)e^{-\alpha\sqrt{s}}-e^{\alpha\sqrt{s}}\left(1+\frac{1}{\sqrt{s}}\right)} \tag{53}$$

The normalized cavity pressure $p/p_{sat}(T_f)$ is $1-g(X=0,\tau)$. Using (51)–(53), the Laplace transform of $g(X=0,\tau)$ is found to be:

$$\tilde{g}(X=0,s)=A+B=\frac{\left(\frac{1-\omega_f}{\sqrt{s}}\right)\sinh(\alpha\sqrt{s})+\frac{c}{s}}{E(s)} \tag{54}$$

where

$$E(s)=\sqrt{s}\sinh(\alpha\sqrt{s})+\cosh(\alpha\sqrt{s}) \tag{55}$$

7.1. Long time and short time behavior

The steady state value of $g(X=0,\tau)$ is determined by the behavior of its transform as $s\to 0$, which is

$$\tilde{g}(X=0,s\to 0)=\frac{c}{s} \tag{56}$$

Eq. (56) implies that

$$\phi(X=0,\tau\to\infty)=1-c\ll 1 \tag{57}$$

Thus, for the case of $c=1$ (the plate is exposed to dry air of zero relative humidity), the cavity pressure goes to zero at long time. The short time behavior of the normalized pressure is determined by the behavior of $\tilde{g}(X=0,s)$ for large s. A simple calculation shows that

$$\tilde{g}(X,s\to\infty)=\frac{\left(\frac{1-\omega_f}{\sqrt{s}}\right)}{\sqrt{s}+1} \tag{58}$$

Comparison of (40) and (58) shows that the short time pressure in the finite plate problem is exactly given by the cavity pressure of an infinitely thick plate. This is to be expected, since the moisture transported to the cavity at short times is from material that is close to the cavity surface.

7.2. Exact solution

The exact solution of $g(X=0,\tau)$ can be obtained using the inversion formula

$$g(X=0,\tau)=\frac{1}{2\pi \mathrm{i}}\int_{\gamma-\mathrm{i}\infty}^{\gamma+\mathrm{i}\infty}\tilde{g}(X=0,s)\mathrm{e}^{s\tau}\,\mathrm{d}s \tag{59}$$

where the integral in (59) is evaluated along any line $\mathrm{Re}\,s=\gamma$ to the right of all singularities of $\tilde{g}(X=0,s)$. The complex path integral (59) can be evaluated using residue theorem, the solution is:

$$g(X=0,\tau)=c+\sum_k \mathrm{Re}\,s[\mathrm{e}^{s\tau}\tilde{g}(X=0,s)]|_{s_k} \tag{60}$$

where $\mathrm{Re}\,s[\mathrm{e}^{s\tau}\tilde{g}(X=0,s)]|_{s_k}$ denotes the residue of $\mathrm{e}^{s\tau}\tilde{g}(X=0,s)$ at s_k and s_k are the singular points of $\tilde{g}(X=0,s)$. The singularities of $\tilde{g}(X,s)$ are located at $s=0$ which is a simple pole, and at the zeroes of $E(s)$. The zeroes of $E(s)$ are the roots of

$$\sqrt{s}\tanh(\alpha\sqrt{s})=-1 \tag{61}$$

Let $z=\alpha\sqrt{s}$, using the identity $\tanh z=-\mathrm{i}\tan(\mathrm{i}z)$, (61) can be rewritten as

$$\mathrm{i}z\tan(\mathrm{i}z)=\alpha \tag{62}$$

where

$$\alpha\equiv L\,\mathrm{d}\omega_\mathrm{f}/h=\frac{LRT_\mathrm{f}\psi_0}{hM_\mathrm{w}p_\mathrm{sat}(T_\mathrm{f})} \tag{63}$$

The factor $\mathrm{d}\omega_\mathrm{f}$=0.94 and hence $\alpha\approx L/h$. Let $u=\mathrm{i}z$, then (63) becomes

$$u\tan u=\alpha \tag{64}$$

It can be readily shown that for real α, (64) has infinitely many simple real zeroes. In addition, if u_k is a zero, so is $-u_k$. Denote these zeroes by $\pm u_k$, where k is a non-negative integer. Since the zeroes of (61) are related to the zeroes of (64) by $s_k=-u_k^2/\alpha^2$, the singularities of $\tilde{g}(X,s)$ are all simple poles. The residues of $\mathrm{e}^{s\tau}\tilde{g}(X=0,s)$ are found to be:

$$\mathrm{Re}\,s[\mathrm{e}^{s\tau}\tilde{g}(X=0,s)]|_{s_k}=2\mathrm{e}^{-u_k^2\tau/\alpha^2}\frac{(1-\omega_\mathrm{f})\frac{\sin(u_k)}{u_k}-\frac{c\alpha}{u_k^2}}{(1+\alpha)\frac{\sin(u_k)}{u_k}+\cos(u_k)} \tag{65}$$

For sufficiently large u, the roots of (64) occur close to $k\pi$, where k is an integer. Using (60) and (65), the normalized concentration is given by

$$\phi(X=0,\tau)=1-c-\sum_k 2\mathrm{e}^{-u_k^2\tau/\alpha^2}\frac{(1-\omega_\mathrm{f})\frac{\sin(u_k)}{u_k}-\frac{c\alpha}{u_k^2}}{(1+\alpha)\frac{\sin(u_k)}{u_k}+\cos(u_k)} \tag{66}$$

Eq. (66) implies that the maximum normalized pressure for a given c depends only on the dimensionless parameters α and ω_f. Since $1-\omega_\mathrm{f}\simeq 1$, the dependence on ω_f is extremely weak. Therefore, for a fixed c, the maximum normalized pressure depends only on α. In particular, for $c=1$, the normalized pressure vanishes at long times. Fig. 6 plots the normalized moisture concentration on the cavity surface versus the normalized time for $c=1$ and different values of parameter α. The infinite plate solution (43) is also plotted in

Fig. 6 as a comparison. Since $\phi(X=0,\tau)$ is also the normalized steam pressure, the plots in Fig. 6 are also the time histories of steam pressure. For each α, the normalized pressure $p/p_{\text{sat}}(T_{\text{f}})$ builds up from its initial value of ω_{f} to its maximum $\phi_{\max}$ at $\tau=\tau_{\max}$. The dependence of the maximum normalized pressure $\phi_{\max}$ on α is shown in Fig. 7. Fig. 7 shows that the maximum pressure increases rapidly for small values of α (thin plates); it then levels out for $\alpha \geqslant 25$. Since $\frac{RT_{\text{f}}\psi_0}{M_{\text{w}}p_{\text{sat}}(T_{\text{f}})} \simeq 1$, the results in Fig. 7 predict that the steam pressure inside the cavity will be close to the saturated vapor pressure if the plate to cavity thickness ratio exceeds 25. This is about six times thicker than the depletion layer in the infinite plate problem. It should be noted that the plate corresponding to $\alpha=25$ is quite thin, it is about 25 times the cavity depth.

Let the normalized time where the normalized pressure *first* reaches 0.9 by τ^* (see Fig. 6). Beyond this time, the pressure reaches a maximum then decreases to 0.9 at $\tau=\tau^{**}$. The difference between these two times, $\Delta\tau \equiv \tau^{**}-\tau^*$ determines how long the pressure in the cavity exceeds $0.9P_{\text{sat}}(T_{\text{f}})$. Fig. 6 shows that τ^* in extremely insensitive to α, as long as $\alpha > 10$. A detailed analysis showed that τ^* decreases very slightly with increasing α. In addition, for $\alpha > 25$, the infinite plate solution is a good approximation to the finite plate solution for normalized pressure below 0.9. On the other hand, τ^{**} and hence $\Delta\tau$ increases rapidly with α. This dependence is shown in Fig. 8.

8. Summary and discussion

The steam pressure inside a microcavity when a moisture saturated polymer composite is rapidly heated is determined using by assuming the chemical potential of water is continuous across the cavity/polymer interface. In this work we consider a single isolated "crack-like" cavity in a composite plate. However, the formulation in this work can be used to compute the moisture content in a composite containing a large number of cavities of different size and shape. The key result in this paper is that maximum steam pressure $p_{\max}$ is a function of a single dimensionless constant α,

$$p_{\max} = p_{\text{sat}}(T_{\text{f}})\phi_{\max}(\alpha) \tag{67}$$

where $\alpha = \frac{LRT_{\text{f}}\psi_0}{hM_{\text{w}}p_{\text{sat}}(T_{\text{f}})}$. It is interesting to note that, with the exception of ψ_0, α is completely determined by the geometry of the composite and the thermodynamic properties of pure water, and is otherwise independent of the properties of the composite (e.g. diffusivity). However, the time needed to reach maximum steam pressure depends on both the diffusivity and α.

Although all the examples in this work are based on the temperature range from 300 and 600 K, which corresponds to $\omega_{\text{f}} = 6.7\times\ 10^{-4}$, the analysis is valid for all temperature ranges.

Our results allow us to establish a condition for blister-induced delamination. Consider a circular cylindrical cavity of radius a. The height of the cavity h is assumed to be much smaller than its radius, i.e., $h/a \ll 1$ so that it can be treated as a penny-shape crack. Assuming that a is much smaller than the typical plate dimension, then the maximum strain energy release rate G due to a uniform pressure loading on the crack faces is:

$$G = \frac{4(1-\nu^2)}{\pi}\frac{[p_{\max}(\alpha)]^2 a}{E} \tag{68}$$

where E and ν is the Young's modulus and Poisson's ratio of the composite plate which is assumed to be isotropic. Fracture of the blister will occur if

$$\frac{4(1-\nu^2)}{\pi}\frac{[p_{\max}(\alpha)]^2 a}{E} = G_{\text{c}} \tag{69}$$

where G_{c} is the fracture toughness of the composite in Mode I. Thus, to prevent blister induced delamination, the maximum steam pressure

$$p_{\max}(\alpha) < \sqrt{EG_c/a}, \tag{70}$$

where we have ignored the factor $4(1-\nu^2)/\pi$. As an example, the maximum steam pressure inside a cavity in a thick composite that is rapidly heated from room temperature to 600 K is about 12 MPa. The critical flaw size computed using (70) with $E = 2.5$ GPa and G_c=40 J/m^2 is about 700 μm. This is a large flaw in comparison with typical defect size in a composite. However, it must be noted that when composites are subjected to hydrothermal fatigue conditions, small flaws can grow sub-critically; that is, crack growth occurs at energy release rates much lower than G_c (Gurumurthy et al., 2002). In addition, the rate of crack growth under these conditions will be sensitive to the duration of high pressure. As shown in Fig. 8, this duration is sensitive to α. Specifically, even if the steam pressure inside thin plates (e.g. $L/h \simeq 25$) can reach the maximum steam pressure, the duration of this pressure is very short; thus sub-critical crack growth is much faster in thick plates. To develop a theory for the safe operation of high temperature composites under these conditions, it is necessary to relate the mechanism of sub-critical crack growth to the local stress and deformation fields.

There are obvious limitations in this work. For example, the composite is heated infinitely fast. This assumption provides an upper bound for the maximum steam pressure inside a cavity. The effect of finite heating rate on the steam pressure will be the subject of an upcoming work.

Our model does not include the effect of stress on the chemical potential, which was considered by Weitsman (1987). Also, the cavity is not deformable, which leads to a more conservative estimate for the steam pressure. We do not expect the effect of stress to be very large, however, since the steam pressure is significantly less than the elastic modulus of the composite. Thus, the change of the dimension of the cavity will be small. Specifically, since the maximum pressure is a function only of α which is inversely proportional to h, a change of h of a few percent should not significantly affect our results. However, the assumption that the activity of water in the polymer obeys Henry's law merits further scrutiny since experiments supporting this result are carried out in a limited temperature range. If Henry's law is not satisfied, the governing equations will be nonlinear and are much more difficult to solve.

Another limitation of our model is the use of the ideal gas law to compute the steam pressure (see (16)). For most gases, including water vapor, the compressibility PV/nRT satisfy a relation of the form

$$PV/nRT = f(P_R, T_R) \tag{71}$$

where f is a universal function independent of gases, $P_R = P/P_c$ and $T_R = T/T_c$ are the reduced pressure and temperature respectively; and we have denoted the critical pressure and temperature by P_c and T_c, respectively (Gaskell, 1981). For $P_R = P/P_c < 1$, f is approximately linear in the reduced pressure, i.e.,

$$PV/nRT = 1 - \beta(T_R)P_R \tag{72}$$

Since the melting temperature of polyimide is close to the critical temperature of water, which is 647.3 K, the condition $T_f < T_c$ is always satisfied. Eq. (72) implies that the ideal gas law underestimates the number of moles of water needed to create a given pressure. For example, at $T = T_f$, (72) implies that the actual number of moles of water needed to sustain the saturated vapor pressure $P_{sat}(T_f)$ is

$$n_{sat} = \frac{[P_{sat}(T_f)V/RT_f]}{[1-\beta(T_f/T_c)(P_{sat}(T_f)/P_c)]} \tag{73}$$

which is *greater* than the ideal gas prediction, $P_{sat}(T_f)V/RT_f$, by a factor of

$$[1-\beta(T_f/T_c)(P_{sat}(T_f)/P_c)]^{-1}$$

At T_f=623 K, this factor is about 2. As a result, the ideal gas assumption underestimates the time for the steam pressure to reach its maximum value. Therefore, the result in this work provides a lower bound for

the time taken for the steam pressure to reach its maximum and an upper bound for the maximum pressure. The effect of non-ideal gas behavior on cavity pressure will be the subject of a future work.

Acknowledgment

This work has been funded through NASA Cooperative Agreement NCC3-994, the "Institute for Future Space Transport" University Research, Engineering and Technology Institute. C.Y. Hui benefited greatly from a private note on moisture diffusion written by Professor E.J. Kramer at the University of California, Santa Barbara. For example, the idea of using Henry's law is Professor Kramer's. He also enjoyed the many discussions with E.J. Kramer on this problem.

References

Bowman, C.L., Sutter, J.K., Thesken, J.C., Rice, B.P., 2001. Characterization of graphite fiber/polyimide composites for RLV applications. In: 46th International SAMPE Symposium and Exhibition, vol. 46(2), pp. 1515–1529.

Deiasi, R., Whiteside, J.B., 1978. Effect of moisture on epoxy resins and composites. In: Vinson, J.R. (Ed.), Advanced Composite Materials-Environmental Effects, ASTM STP 658, pp. 2–20.

Gannamani, R., Pecht, M., 1996. An experimental study of popcorning in plastic encapsulated microcircuits. IEEE Transactions on Components, Packaging and Manufacturing Technology 19 (2), 194–201.

Gaskell, D.R., 1981. Introduction to Metallurgical Thermodynamics, 2nd ed. Hemisphere Publishing Corporation, New York.

Gurumurthy, C.K., Kramer, E.J., Hui, C.Y., 2002. Predicting Crack growth along polymer interfaces due to water attack and thermal fatigue. In: Aliabadi, M.H. (Ed.), Thermomechanical Fatigue and Fracture. WIT Press, Southampton, UK.

Loos, A.C., Springer, G.S., 1981. Moisture absorption of graphite/epoxy composites immersed in liquids and in humid air. In: Springer, G.S. (Ed.), Environmental Effects on Composite Materials. Technomic, vol. 1, pp. 34–50.

McCluskey, P., Munamarty, R., Pecht, M., 1997. Popcorning in PBGA packages during IR reflow soldering. Microelectronics International 42, 20–23.

Price, W.A., Rice, B.P., Crasto, A.S., Thorp, K.A., 1995. Hygrothermal aging of imide composites. In: Proceedings of the High Temple Workshop XV, pp. S1–S24.

Rice, B.P., 1996. Hygrothermal studies on fluorinated polyimides—a physical characterization. In: 28th International SAMPE Technical Conference, pp. 778–789.

Rice, B.P., Lee, C.W., 1997. Study of blister initiation and growth in a high-temperature polyimide. In: 29th International SAMPE Technical Conference, pp. 675–685.

Shewmon, P.G., 1989. Diffusion in solids. Minerals, Metals and Materials Society, Warrendale.

Shirrel, C.D., 1978. Diffusion of water vapor in graphite/epoxy composites. In: Vinson, J.R. (Ed.), Advanced Composite Materials—Environmental Effects. ASTM STP 658, pp. 21–42.

Sullivan, R.M., 1996. The effect of water on thermal stresses in polymer composites. ASME Journal of Applied Mechanics 63, 173–179.

Sullivan, R.M., Stokes, E.H., 1997. A model for the effusion of water in carbon phenolic composites. Mechanics of Materials 26, 197–207.

Weitsman, Y., 1987. Stress assisted diffusion in elastic and viscoelastic materials. Journal of the Mechanics and Physics of Solids 35 (1), 73–93.

Whitney, J.M., Browning, C.E., 1978. Some anomalies associated with moisture diffusion in epoxy matrix composite materials. In: Vinson, J.R. (Ed.), Advanced Composite Materials—Environmental Effects. ASTM STP 658, pp. 43–60.

Woo, M., Piggott, M.R., 1987. Water absorption of resins and composites: I. Epoxy homopolymers and copolymers. Journal of Composites Technology and Research 9 (3), 101–107.